Polymer Journal (2015) 47, 498–504
© 2015 The Society of Polymer Science, Japan (SPSJ) All rights reserved 0032-3896/15
www.nature.com/pj

ORIGINAL ARTICLE

Periodic nanopatterns from polymer blends via directional solidification and subsequent epitaxial crystallization

Xin Zhang, Hirotaka Ejima and Naoko Yoshie

Lamellar patterns with periodicities from several tens to hundreds of nanometers were created by directional solidification and epitaxial crystallization of blends of poly(L-lactide) (PLLA) and poly(vinyl phenol) (PVPh) using hexamethylbenzene as a crystallizable solvent. The effects of blend composition and annealing conditions on both morphologies and periodicities of the patterns were systematically investigated. We show that the morphologies change with the blend composition because the miscibility of the blends and the strength of the hydrogen bonding interaction between PLLA and PVPh depend on the composition and affect the nanoscale phase separation during directional solidification and crystallization. The annealing time required to form well-ordered patterns also depends on the annealing temperature. Overall, we found that blends with 20–30 wt% PVPh annealed at 80 or 100 °C for 30–60 min resulted in well-ordered nanopatterns with tunable periodicity.
Polymer Journal (2015) **47,** 498–504; doi:10.1038/pj.2015.26; published online 13 May 2015

INTRODUCTION

Strategies for fabricating periodically and directionally oriented patterns onto polymer films have drawn great attention from both academia and industry,[1–11] because periodically patterned polymers can be utilized for organic thin-film transistors,[1,2] semiconductor capacitors,[7] magnetic storage devices,[8] nanolithography,[9] organization of nanoparticles[10,11] and other applications. Great efforts have been focused on the fabrication of block copolymers,[12–17] where phase separation is constricted by covalent bonds between the blocks, resulting in nanoscale phase patterns. Micropatterning has also been attempted in polymer blends,[18–23] because the sample preparation process is simpler than that for block copolymer fabrication. However, whereas block copolymers autonomously form thermodynamically stable structures with well-aligned nanopatterns, the phase separation of polymer blends proceeds on a larger scale owing to the absence of covalent bonds between the two polymer blend components. Micro-scale patterning in polymer blends requires structural freezing at an early stage during phase separation. Furthermore, fabrication of directionally oriented polymer blend patterns requires the use of external fields such as prepatterned substrates[18–21] and convection[22,23] to guide the direction of phase separation.

The concept of epitaxy, that is, the growth of a guest crystal on the surface of a host crystal in one or more strictly defined crystallographic orientations, has been applied to patterning with polymer thin films.[24] Crystallization of various polymers on substrate polymers or on small molecules has been investigated. In some cases, epitaxial crystallization has been induced by cooling a hot solution of a polymer in a crystallizable solvent to a temperature below the melting point of the solvent. In such a mixture, the crystals of the solvent act as an epitaxial substrate for the polymer, which is solidified by the loss of the solvent.[24–27] This method also has been applied to semicrystalline diblock copolymers, for which microdomain orientation on relatively large scales has been achieved.[28–32]

Recently, we fabricated well-aligned, nanometer-scale lamellar patterns in a polymer blend of semicrystalline poly(L-lactide) (PLLA) and amorphous poly(vinyl acetate) (PVAc) by means of epitaxial crystallization using a crystallizable solvent, hexamethylbenzene (HMB).[33] In this process, quick directional solidification of the polymer blends restricts the phase separation to the nanometer scale. Epitaxial crystallization of PLLA on HMB generates oriented crystals. This research clearly demonstrated that covalent bonds between component polymers are not crucial for nanopatterning in polymer films. Herein, we apply this method to blends of PLLA and poly(vinyl phenol) (PVPh) to systematically investigate the effective processing conditions for controlling the resulting morphologies. PVPh is partially miscible with PLLA: at low-PVPh content, blends are miscible, but phase separation occurs in blends with high PVPh content.[34–36] The crystallinity of the blend is also reduced severely with increasing PVPh content owing to hydrogen bonding between the hydroxyl group of PVPh and the carbonyl group of PLLA. In this work, we investigated the mechanism of nanopatterning from a blend with relatively strong molecular interaction. Through our examinations of blending ratio and thermal conditions, we demonstrated the effects of PVPh content and annealing temperature on the morphology and periodicity of the nanopatterns fabricated from PLLA/PVPh blends. Consequently, we clarified the conditions for fabricating well-ordered nanopatterns.

Institute of Industrial Science, The University of Tokyo, Tokyo, Japan
Correspondence: Professor N Yoshie, Institute of Industrial Science, The University of Tokyo, 4-6-1 Komaba, Meguro-ku, Tokyo 153-8505, Japan.
E-mail: yoshie@iis.u-tokyo.ac.jp
Received 28 December 2014; revised 25 March 2015; accepted 25 March 2015; published online 13 May 2015

MATERIALS AND METHODS

Materials

PLLA with a weight-average molecular weight (M_w) of 480 kg mol^{-1} was supplied by Mitsui Chemicals (Tokyo, Japan). PVPh with a M_w of 25 kg mol^{-1} was purchased from Sigma-Aldrich (St Louis, MO, USA). These polymers were used without further purification. HMB (99.0%; Tokyo Chemical Industry, Tokyo, Japan) was purified by sublimation before use. Dehydrated tetrahydrofuran was purchased from Kanto Chemical (Tokyo, Japan) and used as received.

Preparation of polymer blend thin films

Glass slides (18 × 18 mm) were first washed with deionized water under sonication and then immersed in Piranha solution (3/1 v/v mixture of 96% sulfuric acid and 30% H_2O_2) for 1 h to remove organic impurities. (CAUTION: Piranha solution can react violently with organic compounds and should be handled with extreme care.) To remove the Piranha solution thoroughly, the glass slides were rinsed with deionized water, sonicated in deionized water for 20 min and then dried in air. Blends of PLLA and PVPh with predetermined mass ratios were dissolved in dehydrated tetrahydrofuran at 70 °C (0.5 wt% total polymers in tetrahydrofuran), were spin-coated onto a washed glass slide at a rate of 2000 r.p.m. for 20 s and were then dried in air overnight to evaporate the residual solvent.

Directional solidification and epitaxial crystallization

Fine powders of HMB (3–5 mg) were scattered evenly on the spin-coated film of the polymer blend. This sample was covered with another glass slide to prevent severe sublimation of HMB during solidification. This sandwiched sample (glass-film-HMB-glass) was placed on a hotplate preheated to 200 °C and held there for ~10–20 s, until HMB melted completely to yield a homogeneous solution of PLLA/PVPh/HMB. The directional solidification of HMB, as well as that of the polymers, was initiated by applying a temperature gradient, which was achieved by slowly pushing the sandwiched sample over the edge of the hotplate with tweezers. As soon as the solidification finished (within several seconds), the sample was transferred to another hotplate preheated to a desired annealing temperature (80, 100 or 120 °C) and held there for a predetermined period of time. Non-annealed samples also were prepared by quenching the sandwiched sample in liquid nitrogen soon after the solidification. After the annealing or quenching process, the sandwiched sample was disassembled, and the substrate with polymer film was put into a vacuum chamber and kept at 50 °C for 5 h to remove HMB by sublimation.

Characterization

Height and phase images of patterns were obtained by an atomic force microscope (Nanocute, SII Nano Technology, Tokyo, Japan) equipped with a self-sensitive microcantilever (PRC-DF40P) in dynamic force mode. Differential scanning calorimetry measurements were performed on a DSC 6220N (SII Nano Technology, Inc) with 3–4 mg of sample. The glass transition temperature (T_g) and melting temperature (T_m) were determined by the heating scan of the sample after quenching from the melt at a rate of 10 °C min^{-1}. Heats of fusion (ΔH_f) were estimated for samples annealed at 80, 100 or 120 °C for a predetermined period (5–900 min) followed by a heating scan at a rate of 10 °C min^{-1}. Spherulite growth of PLLA, as well as HMB crystal growth, was observed on a polarization microscope (Olympus BX51) with a temperature-controlled stage (Linkam 10002). Fourier-transform infrared spectra were obtained by a Thermo Scientific Nicolet iS10 fourier-transform infrared spectrometer equipped with a Thermo Scientific Smart iTR with a diamond crystal. Fourier-transform infrared spectra of solution-casted PLLA/PVPh blend films were recorded over a wavenumber range of 600 – 4000 cm^{-1} with 2 cm^{-1} resolution.

RESULTS AND DISCUSSION

Miscibility and crystallizability of PLLA/PVPh blends

The partial miscibility between PVPh and PLLA was confirmed by measuring T_g (Supplementary Figure S1). The blends exhibited only one T_g, which increased with decreasing PLLA content from 57 to 87 °C. However, once the PLLA content fell below 40 wt%, the T_g values remained constant, suggesting that phase separation was present in those blends. The blends with high PVPh content might have had another T_g, corresponding to the PVPh-rich phase, near the T_g of PVPh (183 °C). However, because the T_g of PVPh is very close to T_m of PLLA, the presence or absence of a second T_g could not be assessed. The T_m of PLLA was gradually lowered by increasing the PVPh fraction, indicating that PVPh had some impact on the crystallization of PLLA.

The intermolecular hydrogen bonding was evidenced from infrared spectra. The vibration stretching of C=O in PLLA in PLLA/PVPh blends shifted from 1759 to 1749 cm^{-1} with increasing PVPh content from 0 to 70 wt% (Supplementary Figure S2). This blend ratio dependence indicates the enhancement of intermolecular hydrogen bonding between PLLA and PVPh.[34,35] The intermolecular hydrogen bonding was reported to be present even at high temperature (~160 °C),[35] which covers the temperature range of annealing in this work.

The enhancement of hydrogen bonding with increasing PVPh in Supplementary Figure S2 was accompanied with decrease of the PLLA crystallizability shown in Figure 1, in which the crystallization rate of PLLA in the blends was analyzed by means of measuring ΔH_f of the 8/2 and 6/4 blends annealed at 80, 100 and 120 °C for 5–900 min. The data in Figure 1 are displayed as the heat per gram of PLLA in the blends and correspond to the relative degree of crystallinity of PLLA. After annealing for 900 min, ΔH_f decreased with increasing PVPh content. This result is consistent with a previous report[34] showing that PLLA crystallinity is reduced by blending PLLA with PVPh. With the increase in PVPh content, the molecular mobility of PLLA was disturbed further owing to hydrogen bonding interactions with PVPh, which reduced the crystallizability of PLLA. The presence of PVPh also slowed the crystallization of PLLA. After annealing for 60 min, which corresponds to the longest annealing time for the polymer blend patterns shown below, ΔH_f of pure PLLA reached its equilibrium value at 120 °C, whereas the blends were still undergoing crystallization. In both 8/2 and 6/4 blends, ΔH_f at 900 min increased with increasing temperature in the range of 80–120 °C. Further, the rate of PLLA crystallization in the blends was much slower at 80 °C than those at 100 and 120 °C, resulting in a further increase of ΔH_f from 60 to 900 min. For the 6/4 samples annealed for 5 min, the ΔH_f of samples annealed at 100 °C had a slightly larger value (0.78 J g^{-1}) than the sample annealed at 120 °C (0.61 J g^{-1}). This is probably because of

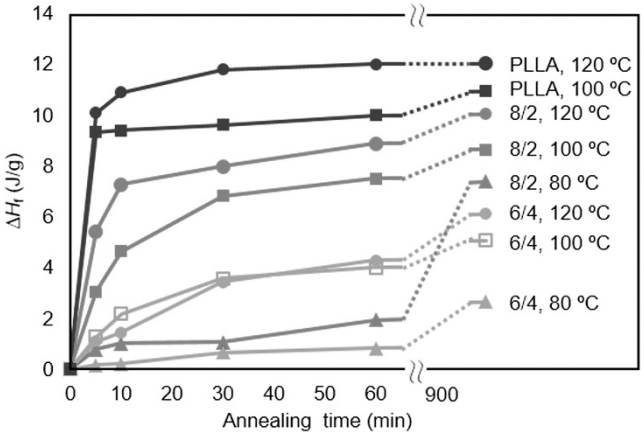

Figure 1 Heat of fusion for PLLA crystalline phase in PLLA/PVPh blends annealed at 80, 100 and 120 °C for 5–60 and 900 min. The data are reported as the heat per gram of PLLA in the blends. A full color version of this figure is available at *Polymer Journal* online.

the faster nucleation at 100 °C in the early stage of annealing than at 120 °C. As the rate of crystal growth in the 6/4 blend was extremely low, the nucleation rate might affect on ΔH_f more significantly than the crystal growth rate does. A parallel investigation of the growth rate of PLLA spherulites in the blends showed similar dependence of the growth rate on the blend composition and the annealing temperature (Supplementary Fig. S3).

Nanopatterning in PLLA/PVPh blends

By an epitaxial crystallization using HMB as a crystallizable solvent, the PLLA/PVPh blends formed nanopatterns with a clear layout and a monodisperse periodicity (Figure 2a–d). The bright domain in the height images, which corresponds to the dark domain in phase images, represents the PLLA crystalline domain.

In the fabrication process adopted in this study, patterning began with a homogenous solution composed of PLLA, PVPh and HMB at 200 °C (Figure 3). A temperature gradient was applied to the solution between flat glass surfaces to induce the crystallization of HMB. The direction of HMB crystal growth (along its *b* axis[32]) was parallel to the direction of the temperature gradient. At the growing front of solidification, where HMB continued transforming from liquid to solid, the polymer concentration concomitantly increased and finally

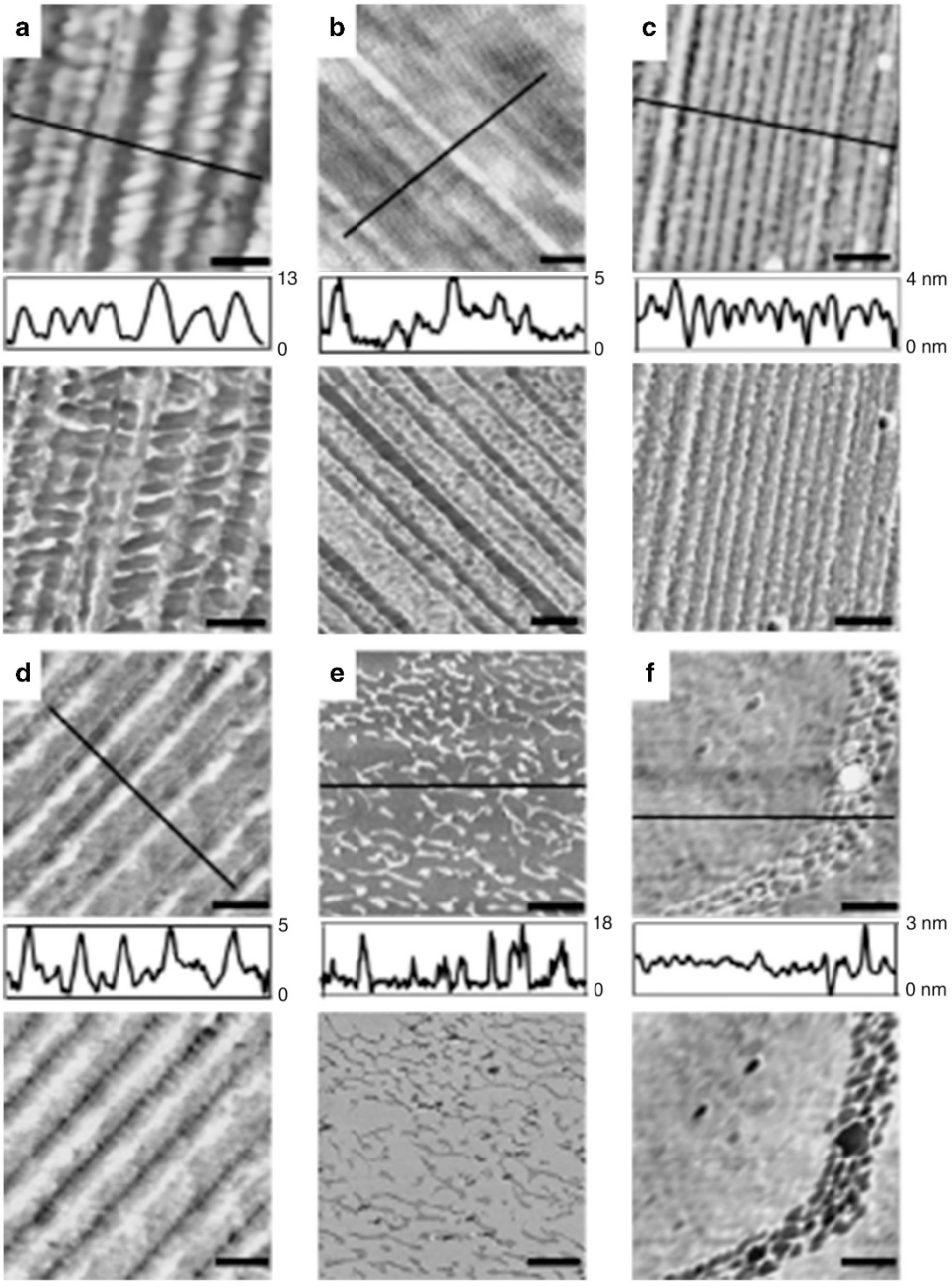

Figure 2 Morphologies of PLLA/PVPh blend thin films visualized by atomic force microscopy (upper panels: height images, bottom panels: phase images). Samples were fabricated by annealing at 80 °C for 60 min. The PLLA/PVPh blends were (**a**) 10/0, (**b**) 9/1, (**c**) 8/2, (**d**) 7/3, (**e**) 5/5 and (**f**) 0/10. The scale bars represent 0.2 μm (**a**–**d**, **f**) and 2.0 μm (**e**). The plots beneath the height images show the depth profiles obtained along the black lines in the corresponding height images. A full color version of this figure is available at *Polymer Journal* online.

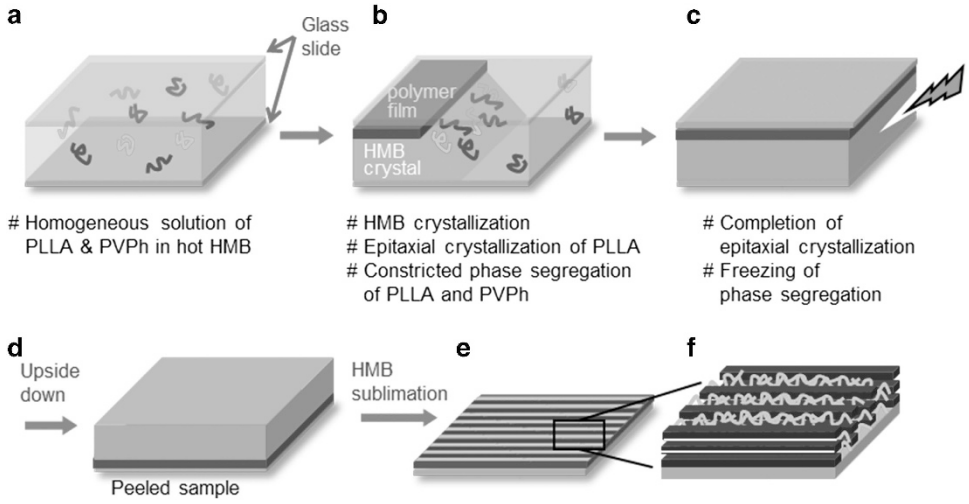

Figure 3 Schematic illustration of the patterning process, including directional solidification and epitaxial crystallization of PLLA/PVPh. (**a**) Homogeneous solution of polymer/HMB at high temperature; (**b**) rapid directional solidification of HMB along the temperature gradient, followed by directional solidification of polymers; (**c**) polymer blend thin films epitaxially crystallized onto HMB crystals; (**d**) the peeled off sample of (**c**), including a polymer layer (in blue) and a HMB layer (in orange); (**e**, **f**) nanostructure of patterned thin film. Lamellar domains (dark blue) represent assembly of PLLA crystalline lamellae. Coils (green) represent amorphous polymers locating in the interlamellar zone. A multilayer structure of crystalline domain is shown in (**f**). A full color version of this figure is available at *Polymer Journal* online.

reached saturation, followed by solidification of polymers. The lamellar pattern might have been nucleated by the shear force of HMB crystallization, which would have forced the polymers to assemble parallel to the *b* axis of HMB, and/or by pinning of the polymers distributed along the extending direction of HMB. During directional solidification, the phase separation in the direction of temperature gradient is not favored because the solidification takes place continuously with a constant polymer ratio at the frontier of liquid–solid transition of polymers. Thus, rather than the direction of temperature gradient, phase separation proceeds in the direction normal to it. This phase separation was frozen and kinetically trapped about ~ 100 nm, because of very rapid growing of HMB crystals. Then, epitaxial crystallization of PLLA eventually proceeded on HMB, with the *c* axis of PLLA vertical to the (001) plane of HMB.[32,37] The subsequent isothermal annealing induced further growth of PLLA crystals, yielding clear and well-ordered nanopatterns. Note that each of the crystalline domains extended into several micrometer or longer in the direction along the temperature gradient. They cannot be one continuously extended single crystal of PLLA. PLLA crystals might form and assemble into the crystalline domains in the lamellar pattern. Further, in the depth direction, a stepped lamellar structure was sometimes observed on the fabricated films (Supplementary Figure S4). This result indicates the multilayer growth of crystalline domains.

Effect of blend composition on the oriented patterns

As shown in Figure 2, well-aligned patterns could be fabricated in PLLA/PVPh with optimized blend compositions of 8/2 and 7/3 (Figure 2c, d). Depth profiles of the patterns showed that well-ordered blend films had a depth range of 3–6 nm, which is smaller than the depth in the pure PLLA sample (Figure 2a). The periodicities of the patterns as estimated by statistical analysis (150–200 data points were collected from images of 10 to 20 separately prepared films) were 153 ± 34 and 76 ± 23 nm for the 7/3 and 8/2 blends, respectively (Figure 4). This difference can be attributed to the increased prevalence of amorphous parts in the 7/3 films compared with that in the 8/2 blend; the amorphous parts enlarged the distance between crystalline domains.

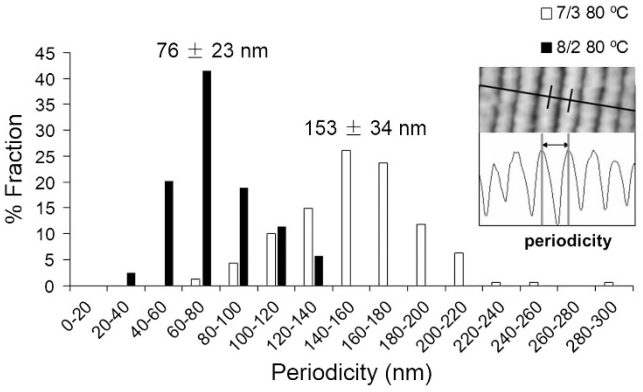

Figure 4 Periodicity distribution of nanopatterns in 8/2 and 7/3 PLLA/PVPh blends. Samples were fabricated by annealing at 80 °C for 60 min. Periodicities were defined as the distance between two peaks of the height profiles, as shown in the inset. The cross line for height profile was set perpendicular to the direction of lamellae. The inset values are the mean ± s.d. ($N = 150$–200). A full color version of this figure is available at *Polymer Journal* online.

In the case of 10/0 films (that is, pure PLLA; Figure 2a), for which there was no driving force for phase separation, the grown crystalline domains were unequal in width, resulting in irregular periodicity. This result suggests that the phase separation induced by the presence of PVPh during the directional solidification is necessary for well-ordered lamellar patterns.

For PVPh content > 50 wt%, we could not obtain aligned lamellar patterns (Figure 2e). With consideration of the closeness between T_g of the 5/5 blend (77 °C) and the annealing temperature for patterning, we also prepared a sample with a higher annealing temperature of 100 °C. Nevertheless, clear patterns could not be obtained; only disordered craters were observed (Supplementary Figure S5). As PLLA and PVPh are miscible in a 5/5 blend, the PLLA molecules are surrounded by PVPh molecules and form hydrogen bonds with them, which would have disturbed the crystallization of PLLA. The reduced crystallizability

observed for this sample could explain the lack of ordered nanopatterns in blends with high PVPh content.

Effect of annealing time and temperature on the oriented patterns

In addition to the PVPh content, the extent of completion of crystallization also substantially affected the evolution of the films into well-ordered nanopatterns. We obtained well-aligned lamellar patterns only when isothermal annealing was applied to induce epitaxial crystallization of PLLA onto HMB. As shown in Figure 5e, a sample prepared without annealing after directional solidification had only crystalline embryos partially organized into elongated lamellar pattern with a low degree of alignment. With increasing annealing time at 80 °C, the periodic morphologies of the patterns gradually evolved. In the image of the 8/2 blend annealed for 5 min (Figure 5a), although the embryos of PLLA crystalline domains tended to align into lamellae, a considerable number of defects were also present. With an additional 5 min annealing, the crystalline domain fused more continuously (Figure 5b). Moreover, the lamellar pattern was more defined as the phase segregation between crystalline and amorphous parts of the film was more complete. After 30 min of annealing (Figure 5c), most of the defects in the film had disappeared and were replaced by lamellar structures. After 60 min, well-ordered patterns with clearly identifiable borders and relatively monodisperse periodicity were eventually formed.

Comparison of the images in Figure 5 clearly shows that evolution into sharper and well-ordered nanopatterns required a certain period of thermal annealing (~60 min for the 8/2 film at 80 °C). This period of annealing would be necessary to complete the epitaxial crystallization of PLLA accompanied by phase segregation between crystalline and amorphous domains.

The 8/2 PLLA/PVPh blends annealed at 100 and 120 °C are shown in Figure 6a–h. Samples prepared at different annealing temperatures required different time periods to complete epitaxial crystallization and lamellar pattern formation. The 8/2 samples annealed at 100 °C did not show any substantial changes in morphology after 30 min, indicating that the periodic patterns formed faster at this temperature than at 80 °C. This temperature dependence of the kinetics of lamellar structure evolution in the thin films is in agreement with the dependence of the spherulite growth rate of the blends (Supplementary Figure S3).

At 120 °C, however, a longer annealing time led to slight deformation of patterns in the 8/2 blend. Compared with the morphology of a sample annealed for 30 min, the morphology of a sample annealed for 60 min contained some defects. (Figure 6g and h). Moreover, the number of defects increased significantly at higher PVPh content (Figure 6l). In the 6/4 blends annealed at 120 °C, the morphology of periodic patterns collapsed at 30 min and disappeared at 60 min (Figure 6i–l). These results occurred probably because the amount of crystallizable PLLA in the blends with higher PVPh content was smaller than the amount in blends with lower PVPh content. The enhanced thermal motion of the amorphous domains may have competed with epitaxial, directional crystal growth at a high annealing temperature.

The periodicity of the 8/2 blend annealed at 100 °C is summarized as a histogram in Figure 7. Compared with the patterns for the sample annealed at 80 °C (Figure 4), the patterns obtained at 100 °C had a wider periodicity. As mentioned above, PLLA crystals grew faster at 100 °C than at 80 °C. The wider periodicity observed for these samples annealed at 100 °C suggests the further phase segregation between crystalline and amorphous domains at 100 °C than at 80 °C.

CONCLUSION

In this study, periodic lamellar nanopatterns were fabricated from polymer blends of PLLA/PVPh through a rapid directional solidification and subsequent epitaxial crystallization of PLLA onto HMB crystals. Effects of blend composition as well as annealing conditions on the morphologies of the patterns were systematically investigated. Blend composition (that is, the ratio of PLLA to PVPh) influenced the patterns' morphologies owing to differences in miscibility and in the strength of hydrogen bonding interactions between the polymers. Optimum ratios (that is, PLLA/PVPh 8/2 or 7/3) yielded well-ordered patterns with monodisperse periodicities, whereas relatively strong

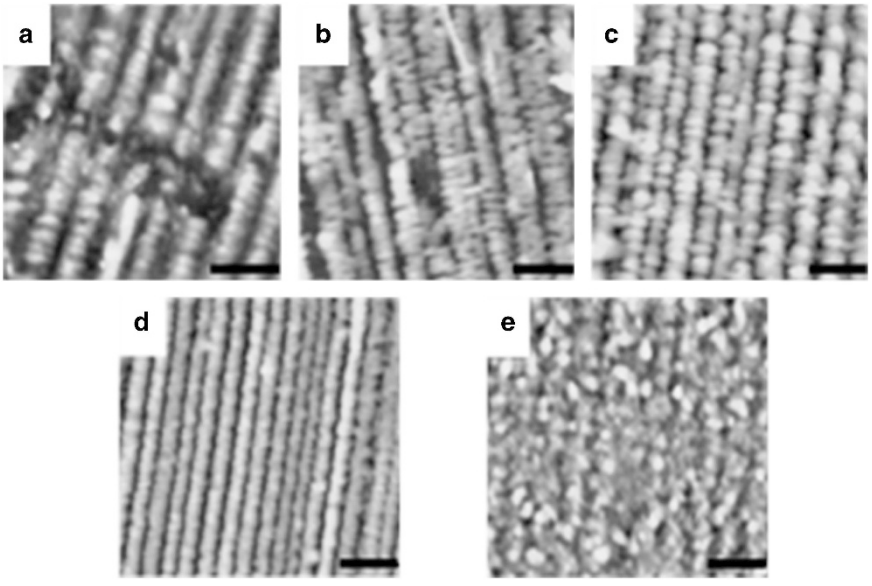

Figure 5 Effect of annealing time on the morphology of the 8/2 PLLA/PVPh blend. Height images of samples annealed at 80 °C for (**a**) 5 min, (**b**) 10 min, (**c**) 30 min and (**d**) 60 min. (**e**) Sample quenched immediately after directional solidification, without annealing. The scale bars represent 0.2 μm. A full color version of this figure is available at *Polymer Journal* online.

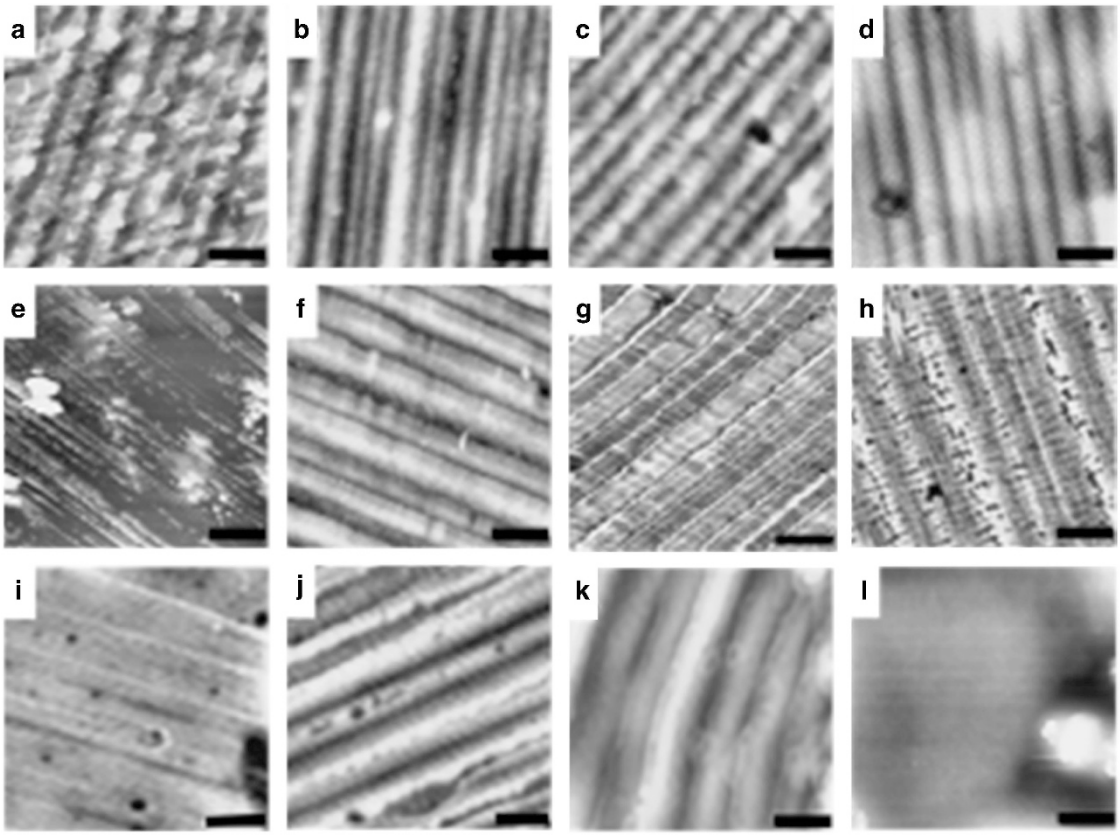

Figure 6 Effect of annealing temperature on the morphology of PLLA/PVPh blends. (**a**–**d**) 8/2 blend annealed at 100 °C, (**e**–**h**) 8/2 blend annealed at 120 °C and (**i**–**l**) 6/4 blend annealed at 120 °C. Samples were annealed for 5 min (**a**, **e**, **i**), 10 min (**b**, **f**, **j**), 30 min (**c**, **g**, **k**) and 60 min (**d**, **h**, **l**), respectively. A full color version of this figure is available at *Polymer Journal* online.

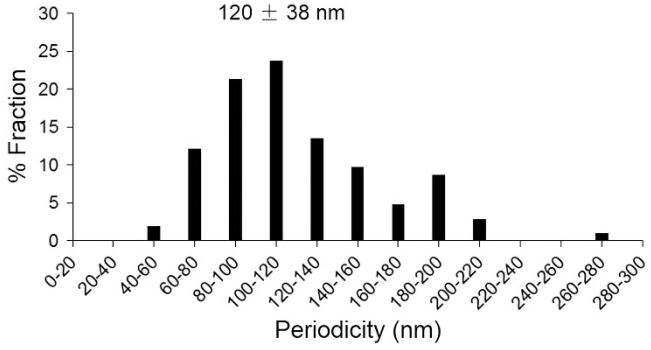

Figure 7 Periodicity distribution of nanopatterns in 8/2 PLLA/PVPh blends annealed at 100 °C. The inset value is the mean ± s.d. ($N = 200$).

hydrogen bonding interactions in blends with high PVPh content (~50 wt%) disrupted the phase separation and reduced the crystallizability of PLLA, resulting in disordered morphologies. Furthermore, the annealing temperature influenced the formation of lamellar structures by altering the growth rate of the PLLA crystals. At high annealing temperature (~120 °C), the effects of thermal motions of amorphous domains became obvious, tending to disturb the periodic lamellar formation. However, by judiciously choosing optimal blend composition, annealing time and annealing temperature, we could create well-ordered nanopatterns that are as promising as those created from block copolymers. This study of nanopatterning of polymer blends having intermolecular hydrogen bonds shows great potential to be applied to a variety of polymers and could offer feasible control over periodicity, both of which remain great challenges for achieving nanometer-scale periodic orientations in polymer thin films.

ACKNOWLEDGEMENTS

This work was financially supported by a grant-in-aid for Scientific Research from Japan Society for the Promotion of Science (KAKENHI No. 25600023). XZ thanks the MEXT Scholarship.

1 Liu, S., Wang, W. M., Briseno, A. L., Mannsfeld, S. C. B. & Bao, Z. N. Controlled deposition of crystalline organic semiconductors for field-effect-transistor applications. *Adv. Mater.* **21**, 1217–1232 (2009).
2 Ling, M. M. & Bao, Z. N. Thin film deposition, patterning, and printing in organic thin film transistors. *Chem. Mater.* **16**, 4824–4840 (2004).
3 Kim, A., Jang, K. S., Kim, J., Won, J. C., Yi, M. H., Kim, H., Yoon, D. K., Shin, T. J., Lee, M. H., Ka, J. W. & Kim, Y. H. Solvent-free directed patterning of a highly ordered liquid crystalline organic semiconductor via template-assisted self-assembly for organic transistors. *Adv. Mater.* **43**, 6219–6225 (2013).
4 Zhou, T. Y., Lin, F., Li, Z. T. & Zhao, X. Single-step solution-phase synthesis of free-standing two-dimensional polymers and their evolution into hollow spheres. *Macromolecules* **46**, 7745–7752 (2013).
5 Bertrand, A. & Hillmyer, M. A. Nanoporous poly(lactide) by olefin metathesis degradation. *J. Am. Chem. Soc.* **135**, 10918–10921 (2013).
6 Zhang, K. D., Tian, J., Hanifi, D., Zhang, Y. B., Sue, A. C. H., Zhou, T. Y., Zhang, L., Zhao, X., Liu, Y. & Li, Z. T. Toward a single-layer two-dimensional honeycomb supramolecular organic framework in water. *J. Am. Chem. Soc.* **135**, 17913–17918 (2013).
7 Black, C. T., Guarini, K. W., Milkove, K. R., Baker, S. M., Russell, T. P. & Tuominen, M. T. Integration of self-assembled diblock copolymers for semiconductor capacitor fabrication. *Appl. Phys. Lett.* **79**, 409–411 (2001).

8 Cheng, J. Y., Ross, C. A., Chan, V. Z. H., Thomas, E. L., Lammertink, R. G. H. & Vancso, G. J. Formation of a cobalt magnetic dot array via block copolymer lithography. *Adv. Mater.* **13**, 1174–1178 (2001).
9 Park, M., Harrison, C., Chaikin, P. M., Register, R. A. & Adamson, D. H. Block copolymer lithography: periodic arrays of ~10^{11} holes in 1 square centimeter. *Science* **276**, 1401–1404 (1997).
10 Zhao, Y., Thorkelsson, K., Mastroianni, A. J., Schilling, T., Luther, J. M., Rancatore, B., Matsunaga, K., Jinnai, H., Wu, Y., Poulsen, D., Fréchet, J. M. J., Alivisatos, A. P. & Xu, T. Small-molecule-directed nanoparticle assembly towards stimuli-responsive nanocomposites. *Nat. Mater.* **8**, 979–985 (2009).
11 Jang, S. G., Khan, A., Hawker, C. J. & Kramer, E. J. Morphology evolution of PS-*b*-P2VP diblock copolymers via supramolecular assembly of hydroxylated gold nanoparticles. *Macromolecules* **45**, 1553–1561 (2012).
12 Bates, F. S. & Fredrickson, G. H. Block copolymer thermodynamics: theory and experiment. *Annu. Rev. Phys. Chem.* **41**, 525–557 (1990).
13 Segalman, R. A. Patterning with block copolymer thin films. *Mater. Sci. Eng.* **48**, 191–226 (2005).
14 Matsushita, Y. Creation of hierarchically ordered nanophase structures in block polymers having various competing interactions. *Macromolecules* **40**, 771–776 (2007).
15 Stoykovich, M. P., Müller, M., Kim, S. O., Solak, H. H., Edwards, E. W., de Pablo, J. J. & Nealey, P. F. Directed assembly of block copolymer blends into nonregular device-oriented structures. *Science* **308**, 1442–1446 (2005).
16 Jeong, J. W., Park, W. I., Do, L. M., Park, J. H., Kim, T. H., Chae, G. & Jung, Y. S. Nanotransfer printing with sub-10 nm resolution realized using directed self-assembly. *Adv. Mater.* **24**, 3526–3531 (2012).
17 Keen, I., Cheng, H. H., Yu, A., Jack, K. S., Younkin, T. R., Leeson, M. J., Whittaker, A. K. & Blakey, I. Behavior of lamellar forming block copolymers under nanoconfinement: implications for topography directed self-assembly of sub-10 nm structures. *Macromolecules* **47**, 276–283 (2014).
18 Böltau, M., Walheim, S., Mlynek, J., Krausch, G. & Steiner, U. Surface-induced structure formation of polymer blends on patterned substrates. *Nature* **391**, 877–879 (1998).
19 Rockford, L., Liu, Y., Mansky, P., Russell, T. P., Yoon, M. & Mochrie, S. G. J. Polymers on nanoperiodic, heterogeneous surfaces. *Phys. Rev. Lett.* **82**, 2602–2605 (1999).
20 Coffey, D. C. & Ginger, D. S. Patterning phase separation in polymer films with dip-pen nanolithography. *J. Am. Chem. Soc.* **127**, 4564–4565 (2005).
21 Fang, L., Wei, M., Shang, Y., Kazmer, D., Barry, C. & Mead, J. Precise pattern replication of polymer blends into nonuniform geometries via reducing interfacial tension between two polymers. *Langmuir* **28**, 10238–10245 (2012).
22 Wu, K. H., Lu, S. Y. & Chen, H. L. Formation of parallel strips in thin films of polystyrene/poly(vinyl pyrrolidone) blends via spin coating on unpatterned substrates. *Langmuir* **22**, 8029–8035 (2006).
23 Byun, M., Hong, S. W., Qiu, F., Zou, Q. & Lin, Z. Evaporative organization of hierarchically structured polymer blend rings. *Macromolecules* **41**, 9312–9317 (2008).
24 Wittmann, J. C. & Lotz, B. Epitaxial crystallization of polymers on organic and polymeric substrates. *Prog. Polym. Sci.* **15**, 909–948 (1990).
25 Zwiers, R. J. M., Gogolewski, S. & Pennings, A. J. General crystallization behaviour of poly(L-lactic acid) PLLA: 2. Eutectic crystallization of PLLA. *Polymer* **24**, 167–174 (1983).
26 Zuo, Z. C., Yin, X. D., Zhou, C. J., Chen, N., Liu, H. B., Li, Y. J. & Li, Y. L. Organic crystallizable solvent served as template for constructing well-ordered PPE films. *J. Colloid Interface Sci.* **356**, 86–91 (2011).
27 Da Costa, V., Le Moigne, J., Oswald, L., Pham, T. A. & Thierry, A. Thin film orientation by epitaxy of carbazolyl polydiacetylenes: guest – host interaction on a crystal surface. *Macromolecules* **31**, 1635–1643 (1998).
28 De Rosa, C., Park, C., Thomas, E. L. & Lotz, B. Microdomain patterns from directional eutectic solidification and epitaxy. *Nature* **405**, 433–437 (2000).
29 De Rosa, C., Park, C., Lotz, B., Wittmann, J. C., Fetters, L. J. & Thomas, E. L. Control of molecular and microdomain orientation in a semicrystalline block copolymer thin film by epitaxy. *Macromolecules* **33**, 4871–4876 (2000).
30 Cartier, L., Okihara, T., Ikada, Y., Tsuji, H., Puiggali, J. & Lotz, B. Epitaxial crystallization and crystalline polymorphism of polylactides. *Polymer* **41**, 8909–8919 (2000).
31 Park, C., De Rosa, C. & Thomas, E. L. Large area orientation of block copolymer microdomains in thin films via directional crystallization of a solvent. *Macromolecules* **34**, 2602–2606 (2001).
32 Tseng, W. H., Hsieh, P. Y., Ho, R. M., Huang, B. H., Lin, C. C. & Lotz, B. Oriented microstructures of polystyrene-*b*-poly(L-lactide) thin films induced by crystallizable solvents. *Macromolecules* **39**, 7071–7077 (2006).
33 Ejima, H., Itako, J. E., Ishida, K. & Yoshie, N. Nanostructured thin films of polymer blends by directional crystallization onto crystallizable organic solvent. *Macromolecules* **40**, 6445–6447 (2007).
34 Zhang, L. L., Goh, S. H. & Lee, S. Y. Miscibility and crystallization behaviour of poly(L-lactide)/poly(p-vinylphenol) blends. *Polymer* **39**, 4841–4847 (1998).
35 Meaurio, E., Zuza, E. & Sarasua, J. R. Miscibility and specific interactions in blends of poly(L-lactide) with poly(vinylphenol). *Macromolecules* **38**, 1207–1215 (2005).
36 Meaurio, E., Zuza, E. & Sarasua, J. R. Direct measurement of the enthalpy of mixing in miscible blends of poly(DL-lactide) with poly(vinylphenol). *Macromolecules* **38**, 9221–9228 (2005).
37 Lonsdale, K. The structure of the benzene ring in $C_6(CH_3)_6$. *Proc. Roy. Soc. A* **123**, 494–515 (1929).

Supplementary Information accompanies the paper on Polymer Journal website (http://www.nature.com/pj)